

Distinguishing between the twin b -flavored unitarity triangles on a circular arc

Zhi-zhong Xing^{1,2} * and Di Zhang¹ †

¹Institute of High Energy Physics and School of Physical Sciences,
University of Chinese Academy of Sciences, Beijing 100049, China

²Center of High Energy Physics, Peking University, Beijing 100871, China

Abstract

With the help of the generalized Wolfenstein parametrization of quark flavor mixing and CP violation, we calculate fine differences between the twin b -flavored unitarity triangles defined by $V_{ub}^*V_{ud} + V_{cb}^*V_{cd} + V_{tb}^*V_{td} = 0$ and $V_{ud}^*V_{td} + V_{us}^*V_{ts} + V_{ub}^*V_{tb} = 0$ in the complex plane. We find that vertices of the rescaled versions of these two triangles, described respectively by $\bar{\rho} + i\bar{\eta} = -(V_{ub}^*V_{ud}) / (V_{cb}^*V_{cd})$ and $\tilde{\rho} + i\tilde{\eta} = -(V_{ub}^*V_{tb}) / (V_{us}^*V_{ts})$, are located on a circular arc whose center and radius are given by $O = (0.5, 0.5 \cot \alpha)$ and $R = 0.5 \csc \alpha$ with α being their common inner angle. The small difference between $(\bar{\rho}, \bar{\eta})$ and $(\tilde{\rho}, \tilde{\eta})$ is characterized by $\tilde{\rho} - \bar{\rho} \sim \tilde{\eta} - \bar{\eta} \sim \mathcal{O}(\lambda^2)$ with $\lambda \simeq 0.22$ being the Wolfenstein expansion parameter, and these two vertices are insensitive to the two-loop renormalization-group running effects up to the accuracy of $\mathcal{O}(\lambda^4)$. Some comments are also made on similar features of three pairs of the rescaled unitarity triangles of lepton flavor mixing and CP violation.

arXiv:1911.03292v1 [hep-ph] 8 Nov 2019

*E-mail: xingzz@ihep.ac.cn

†E-mail: zhangdi@ihep.ac.cn (corresponding author)

1 Introduction

The running Belle II detector at the KEK super-B factory [1] and an upgrade of the LHCb detector at CERN [2, 3] are pushing B -meson physics and CP violation into a new era, in which further precision measurements will be done to test the standard model (SM) predictions for b -flavored hadrons to an unprecedented degree of accuracy and probe possible new physics via their fine quantum corrections to the SM results. An intriguing question is whether these two experiments can finally distinguish between the following *twin* b -flavored unitarity triangles of the Cabibbo-Kobayashi-Maskawa (CKM) quark flavor mixing matrix V [4, 5] in the complex plane:

$$\begin{aligned}\Delta_s &: V_{ub}^* V_{ud} + V_{cb}^* V_{cd} + V_{tb}^* V_{td} = 0, \\ \Delta_c &: V_{ud}^* V_{td} + V_{us}^* V_{ts} + V_{ub}^* V_{tb} = 0,\end{aligned}\tag{1}$$

where each triangle is named after the flavor index that does not appear in its three sides [6, 7]. The reason is simply that these two triangles are almost congruent with each other, and hence their differences in sides and inner angles are experimentally indistinguishable at present. Notice that the triangle Δ_s has played a crucial role in verifying the success of the Kobayashi-Maskawa mechanism of CP violation, and it has been extensively studied in various decays of B_d and B_u mesons in the past twenty years. In comparison, the triangle Δ_c seems to have a much closer relationship with the B_s -meson decays, so its sides and inner angles are expected to be carefully measured in the next twenty years at the LHCb and Belle II experiments. Needless to say, an experimental confirmation of high similarity between Δ_c and Δ_s will provide us with stronger evidence for correctness of the SM in the quark flavor mixing sector, while a discovery of some unexpected and unsuppressed differences between these twin triangles will serve as a remarkable signal of new physics beyond the SM. Such a point was already emphasized by Bigi and Sanda two decades ago [8], and *now it is time for us to confront it with the upcoming measurements at the super-B factory and the high-luminosity Large Hadron Collider (LHC)*.

The main purpose of this work is two-fold. On the one hand, we are going to carry out a careful study of fine differences between the *rescaled* versions of Δ_s and Δ_c ,

$$\begin{aligned}\Delta'_s &: 1 + \frac{V_{ub}^* V_{ud}}{V_{cb}^* V_{cd}} + \frac{V_{tb}^* V_{td}}{V_{cb}^* V_{cd}} = 0, \\ \Delta'_c &: 1 + \frac{V_{ud}^* V_{td}}{V_{us}^* V_{ts}} + \frac{V_{ub}^* V_{tb}}{V_{us}^* V_{ts}} = 0,\end{aligned}\tag{2}$$

with the help of the Wolfenstein parametrization of V [9]. On the other hand, we shall examine the stability of Δ'_s and Δ'_c against quantum corrections by using the two-loop renormalization-group equations (RGEs) of the CKM matrix V [10, 11, 12, 13]. Analogous to the definition

$$\bar{\rho} + i\bar{\eta} = -\frac{V_{ub}^* V_{ud}}{V_{cb}^* V_{cd}}\tag{3}$$

for the vertex of Δ'_s [14, 15, 16], the vertex of Δ'_c can be defined as

$$\tilde{\rho} + i\tilde{\eta} = -\frac{V_{ub}^* V_{tb}}{V_{us}^* V_{ts}}\tag{4}$$

in the complex plane. The analytical expressions of $(\bar{\rho}, \bar{\eta})$ and $(\tilde{\rho}, \tilde{\eta})$ will be derived up to the accuracy of $\mathcal{O}(\lambda^6)$, where $\lambda \simeq 0.22$ is the Wolfenstein expansion parameter, so as to see the tiny difference between these two rescaled unitarity triangles. We find that the vertices $(\bar{\rho}, \bar{\eta})$ and $(\tilde{\rho}, \tilde{\eta})$ are actually located on a circular arc in the complex plane. Both $\tilde{\rho} - \bar{\rho}$ and $\tilde{\eta} - \bar{\eta}$ are of

$\mathcal{O}(\lambda^2)$, and thus Δ'_c and Δ'_s should be experimentally distinguishable if their vertices $(\bar{\rho}, \bar{\eta})$ and $(\tilde{\rho}, \tilde{\eta})$ can be measured at the 1% precision level. The similar experimental sensitivity will allow us to probe small differences between the inner angles of Δ'_c and Δ'_s . We also find that $(\bar{\rho}, \bar{\eta})$ and $(\tilde{\rho}, \tilde{\eta})$ are insensitive to the two-loop RGE running effects up to the accuracy of $\mathcal{O}(\lambda^4)$, implying that the shapes of Δ_c and Δ_s keep invariant up to the same accuracy when the energy scale evolves from the electroweak scale $\Lambda_{\text{EW}} \sim 10^2$ GeV to the scale of a grand unification theory (GUT) — $\Lambda_{\text{GUT}} \sim 10^{16}$ GeV (or vice versa). Therefore, the experimental results of all the inner angles of Δ_c and Δ_s obtained at low energies can directly be confronted with some theoretical predictions at a superhigh energy scale. We finally make some brief comments on similar features of three pairs of the rescaled unitarity triangles of lepton flavor mixing and CP violation in the complex plane, which are expected to be useful for the study of neutrino oscillations.

2 The vertices of Δ'_s and Δ'_c on a circular arc

Let us start from a popular extension of the original Wolfenstein parametrization of the CKM matrix V proposed by Buras *et al* in 1994 [14, 15, 16]. Since $\mathcal{O}(\lambda^6)$ is equivalent to $\mathcal{O}(10^{-4})$, it is good enough for us to expand each element of V in powers of λ up to this degree of accuracy. To be explicit, one actually finds $V_{us} = \lambda + \mathcal{O}(\lambda^7)$, $V_{cb} = A\lambda^2 + \mathcal{O}(\lambda^8)$ and $V_{ub} = A\lambda^3(\rho - i\eta)$, together with

$$\begin{aligned}
V_{ud} &= 1 - \frac{1}{2}\lambda - \frac{1}{8}\lambda^4 + \mathcal{O}(\lambda^6), \\
V_{cd} &= -\lambda + \frac{1}{2}A^2\lambda^5 [1 - 2(\rho + i\eta)] + \mathcal{O}(\lambda^7), \\
V_{cs} &= 1 - \frac{1}{2}\lambda^2 - \frac{1}{8}\lambda^4 (1 + 4A^2) + \mathcal{O}(\lambda^6), \\
V_{td} &= A\lambda^3 (1 - \rho - i\eta) + \frac{1}{2}A\lambda^5 (\rho + i\eta) + \mathcal{O}(\lambda^7), \\
V_{ts} &= -A\lambda^2 + \frac{1}{2}A\lambda^4 [1 - 2(\rho + i\eta)] + \mathcal{O}(\lambda^6), \\
V_{tb} &= 1 - \frac{1}{2}A^2\lambda^4 + \mathcal{O}(\lambda^6).
\end{aligned} \tag{5}$$

Substituting the above expressions into Eq. (3) and Eq. (4), we directly arrive at

$$\begin{aligned}
\bar{\rho} &= \rho \left\{ 1 - \frac{1}{2}\lambda^2 - \left[\frac{1}{8} - \left(\frac{1}{2} - \rho + \frac{\eta^2}{\rho} \right) A^2 \right] \lambda^4 \right\} + \mathcal{O}(\lambda^6), \\
\bar{\eta} &= \eta \left\{ 1 - \frac{1}{2}\lambda^2 - \left[\frac{1}{8} - \left(\frac{1}{2} - 2\rho \right) A^2 \right] \lambda^4 \right\} + \mathcal{O}(\lambda^6);
\end{aligned} \tag{6}$$

and

$$\begin{aligned}
\tilde{\rho} &= \rho \left\{ 1 + \left(\frac{1}{2} - \rho + \frac{\eta^2}{\rho} \right) \lambda^2 + \left[\frac{3}{8} - \frac{1}{2}A^2 - \rho(1 - \rho) - 3\eta^2 + \frac{\eta^2}{\rho} \right] \lambda^4 \right\} + \mathcal{O}(\lambda^6), \\
\tilde{\eta} &= \eta \left\{ 1 + \left(\frac{1}{2} - 2\rho \right) \lambda^2 + \left[\frac{3}{8} - \frac{1}{2}A^2 - \eta^2 - (2 - 3\rho)\rho \right] \lambda^4 \right\} + \mathcal{O}(\lambda^6).
\end{aligned} \tag{7}$$

It is clear that $\tilde{\rho} \simeq \bar{\rho} \simeq \rho$ and $\tilde{\eta} \simeq \bar{\eta} \simeq \eta$ hold in the leading-order approximation, implying a congruence between the rescaled unitarity triangles Δ'_c and Δ'_s . The analytical approximations made in Eqs. (6) and (7) allow us to see some fine differences between the vertices $(\bar{\rho}, \bar{\eta})$ and $(\tilde{\rho}, \tilde{\eta})$ of these two triangles as follows:

$$\tilde{\rho} - \bar{\rho} \simeq [\rho(1 - \rho) + \eta^2] \lambda^2, \quad \tilde{\eta} - \bar{\eta} \simeq \eta(1 - 2\rho) \lambda^2, \tag{8}$$

up to the accuracy of $\mathcal{O}(\lambda^4)$. Given the central values of λ , A , $\bar{\rho}$ and $\bar{\eta}$ which have been determined from a global analysis of current experimental data on quark flavor mixing and CP violation [16],

$$\lambda = 0.22453, \quad A = 0.836, \quad \bar{\rho} = 0.122, \quad \bar{\eta} = 0.355, \quad (9)$$

we find $\rho \simeq 0.125$ and $\eta \simeq 0.364$ from the exact relationship between (ρ, η) and $(\bar{\rho}, \bar{\eta})$ [14, 15, 16]:

$$\rho + i\eta = \frac{\sqrt{1 - A^2\lambda^4}(\bar{\rho} + i\bar{\eta})}{\sqrt{1 - \lambda^2}[1 - A^2\lambda^4(\bar{\rho} + i\bar{\eta})]}. \quad (10)$$

As a result, $\tilde{\rho} \simeq 0.134$ and $\tilde{\eta} \simeq 0.368$ can be obtained from Eq. (7). The differences $\tilde{\rho} - \bar{\rho} \simeq 0.012$ and $\tilde{\eta} - \bar{\eta} \simeq 0.013$ mean that the twin triangles Δ'_c and Δ'_s will be experimentally distinguishable if their vertices $(\bar{\rho}, \bar{\eta})$ and $(\tilde{\rho}, \tilde{\eta})$ can be determined at the 1% precision level.

We proceed to take a look at the inner angles of triangles Δ'_s and Δ'_c . Up to the accuracy of $\mathcal{O}(\lambda^6)$, we obtain

$$\begin{aligned} \alpha &\equiv \arg\left(-\frac{V_{tb}^*V_{td}}{V_{ub}^*V_{ud}}\right) = \arg\left(-\frac{1 - \bar{\rho} - i\bar{\eta}}{\bar{\rho} + i\bar{\eta}}\right) = \arctan\left(\frac{\eta}{\eta^2 + \rho^2 - \rho}\right) + \frac{\eta}{2[\eta^2 + (\rho - 1)^2]}\lambda^2 \\ &\quad + \left\{\frac{\eta(4A^2 + 3)}{8[\eta^2 + (\rho - 1)^2]} - \frac{\eta(1 - \rho)}{4[\eta^2 + (\rho - 1)^2]^2}\right\}\lambda^4 + \mathcal{O}(\lambda^6), \\ \beta &\equiv \arg\left(-\frac{V_{cb}^*V_{cd}}{V_{tb}^*V_{td}}\right) = \arg\left(\frac{1}{1 - \bar{\rho} - i\bar{\eta}}\right) = \arctan\left(\frac{\eta}{1 - \rho}\right) - \frac{\eta}{2[\eta^2 + (\rho - 1)^2]}\lambda^2 \\ &\quad + \left\{\eta A^2 - \frac{\eta(4A^2 + 3)}{8[\eta^2 + (\rho - 1)^2]} + \frac{\eta(1 - \rho)}{4[\eta^2 + (\rho - 1)^2]^2}\right\}\lambda^4 + \mathcal{O}(\lambda^6), \\ \gamma &\equiv \arg\left(-\frac{V_{ub}^*V_{ud}}{V_{cb}^*V_{cd}}\right) = \arg(\bar{\rho} + i\bar{\eta}) = \arctan\left(\frac{\eta}{\rho}\right) - \eta A^2\lambda^4 + \mathcal{O}(\lambda^6); \end{aligned} \quad (11)$$

and

$$\begin{aligned} \alpha' &\equiv \arg\left(-\frac{V_{ud}^*V_{td}}{V_{ub}^*V_{tb}}\right) = \arg\left(-\frac{1 - \tilde{\rho} - i\tilde{\eta}}{\tilde{\rho} + i\tilde{\eta}}\right) = \arctan\left(\frac{\eta}{\eta^2 + \rho^2 - \rho}\right) + \frac{\eta}{2[\eta^2 + (\rho - 1)^2]}\lambda^2 \\ &\quad + \left\{\frac{\eta(4A^2 + 3)}{8[\eta^2 + (\rho - 1)^2]} - \frac{\eta(1 - \rho)}{4[\eta^2 + (\rho - 1)^2]^2}\right\}\lambda^4 + \mathcal{O}(\lambda^6), \\ \beta' &\equiv \arg\left(-\frac{V_{us}^*V_{ts}}{V_{ud}^*V_{td}}\right) = \arg\left(\frac{1}{1 - \tilde{\rho} - i\tilde{\eta}}\right) = \arctan\left(\frac{\eta}{1 - \rho}\right) + \left\{\eta - \frac{\eta}{2[\eta^2 + (\rho - 1)^2]}\right\}\lambda^2 \\ &\quad - \left\{\frac{\eta(4A^2 + 3)}{8[\eta^2 + (\rho - 1)^2]} - \frac{\eta(1 - \rho)}{4[\eta^2 + (\rho - 1)^2]^2} - \eta\left(\frac{1}{2} - \rho\right)\right\}\lambda^4 + \mathcal{O}(\lambda^6), \\ \gamma' &\equiv \arg\left(-\frac{V_{ub}^*V_{tb}}{V_{us}^*V_{ts}}\right) = \arg(\tilde{\rho} + i\tilde{\eta}) = \arctan\left(\frac{\eta}{\rho}\right) - \eta\lambda^2 - \eta\left(\frac{1}{2} - \rho\right)\lambda^4 + \mathcal{O}(\lambda^6). \end{aligned} \quad (12)$$

One can see that $\alpha' = \alpha$ holds exactly, and

$$\beta' - \beta = \gamma - \gamma' \simeq \eta\lambda^2 \left[1 + \left(\frac{1}{2} - A^2 - \rho\right)\lambda^2\right]. \quad (13)$$

So we arrive at $\beta' > \beta$ and $\gamma > \gamma'$, and the difference between each pair of these inner angles is measured by $\eta\lambda^2$ in the leading-order approximation. Taking account of the best-fit values of λ ,

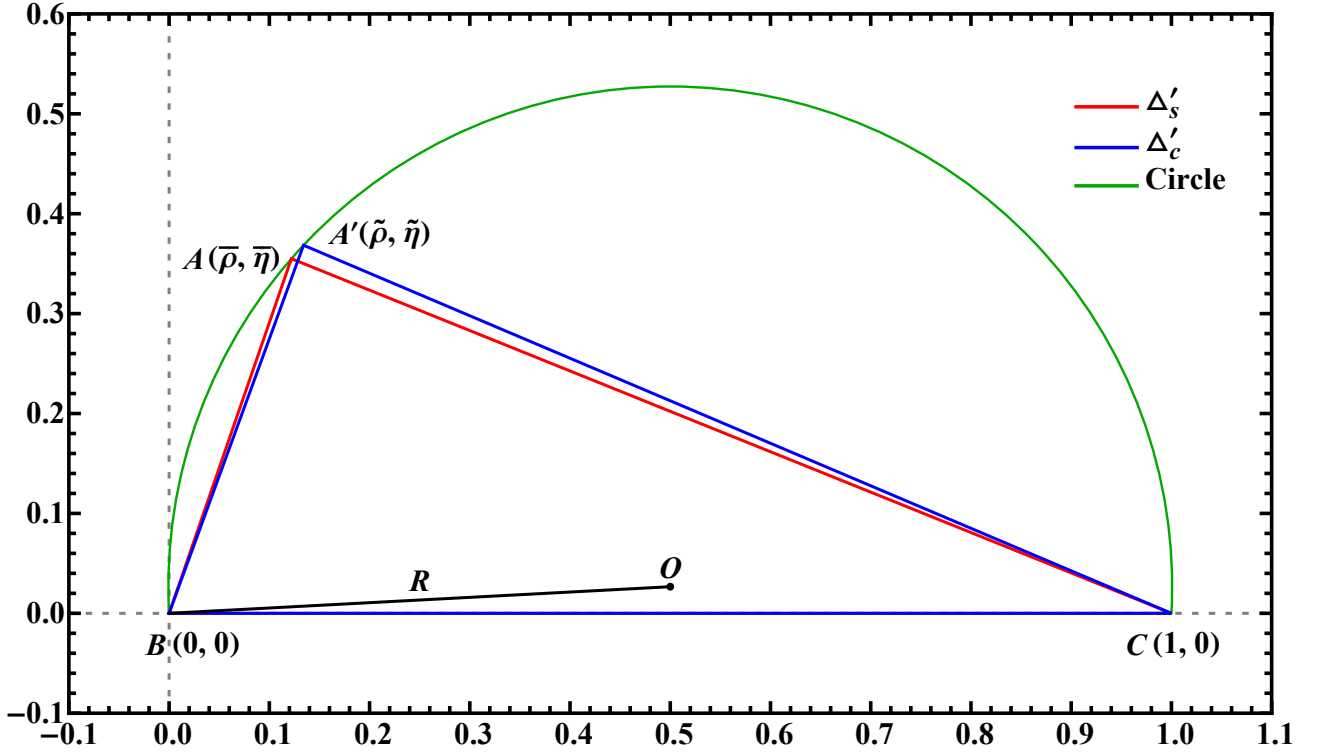


Figure 1: The rescaled CKM unitarity triangles $\Delta'_s = \triangle ABC$ and $\Delta'_c = \triangle A'BC$ in the complex plane, and their corresponding inner angles are defined as $\alpha = \angle BAC$, $\beta = \angle ACB$, $\gamma = \angle ABC$ and $\alpha' = \angle BA'C$, $\beta' = \angle A'CB$, $\gamma' = \angle A'BC$. Note that $\alpha' = \alpha$ holds by definition, as shown in Eqs. (11) and (12). The vertices $A(\bar{\rho}, \bar{\eta})$ and $A'(\tilde{\rho}, \tilde{\eta})$ of these two triangles are located on the same circular arc, whose center and radius are $O = (0.5, 0.5 \cot \alpha)$ and $R = 0.5 \csc \alpha$ respectively.

A , $\bar{\rho}$ and $\bar{\eta}$ in Eq. (9), we immediately obtain $\alpha = \alpha' \simeq 87.0^\circ$, $\beta \simeq 22.0^\circ$, $\gamma \simeq 71.0^\circ$, $\beta' \simeq 23.0^\circ$ and $\gamma' \simeq 70.0^\circ$. Therefore, $\beta' - \beta = \gamma - \gamma' \simeq 1.0^\circ$ characterizes the tiny difference between triangles Δ'_s and Δ'_c in their inner angles.

Now that the twin rescaled unitarity triangles Δ'_c and Δ'_s share a common inner angle $\alpha' = \alpha$ and a common side BC as shown in Figure 1, their corresponding vertices $(\tilde{\rho}, \tilde{\eta})$ and $(\bar{\rho}, \bar{\eta})$ must be on a circular arc in the upper complex plane. To see this interesting point in a more transparent way, let us first write out

$$\cos \alpha = \frac{\bar{\rho}^2 + \bar{\eta}^2 + (1 - \bar{\rho})^2 + \bar{\eta}^2 - 1}{2\sqrt{\bar{\rho}^2 + \bar{\eta}^2}\sqrt{(1 - \bar{\rho})^2 + \bar{\eta}^2}} \quad (14)$$

for vertex $(\bar{\rho}, \bar{\eta})$ with the help of the cosine theorem, and then express this equation as

$$\left(\bar{\rho} - \frac{1}{2}\right)^2 + \left(\bar{\eta} - \frac{1}{2} \cot \alpha\right)^2 = \left(\frac{1}{2} \csc \alpha\right)^2. \quad (15)$$

It becomes obvious that Eq. (14) or (15) actually defines a circular arc in the upper complex plane, whose center and radius are $O = (0.5, 0.5 \cot \alpha)$ and $R = 0.5 \csc \alpha$ respectively. Because Eqs. (14) and (15) keep unchanged with the replacements $\bar{\rho} \rightarrow \tilde{\rho}$ and $\bar{\eta} \rightarrow \tilde{\eta}$, vertex $(\tilde{\rho}, \tilde{\eta})$ must be located on the same circular arc. This observation geometrically illustrates how similar Δ'_c and Δ'_s are, and it can be extended to similar discussions about the other two pairs of the CKM unitarity triangles, whose shapes are nevertheless very sharp [7].

The fact that all the vertices of Δ'_c and Δ'_s are located on the same circular arc is of course a natural consequence of unitarity of the CKM matrix V . It provides another interesting way to test the consistency of quark flavor mixing and CP violation in the SM. Since Δ'_s has been established to a very good degree of accuracy, it allows us to fix a benchmark circular arc as shown in Figure 1. The future measurements of $(\tilde{\rho}, \tilde{\eta})$ will tell us to what extent the experimental values of this vertex are also located on the same circular arc. In other words, an experimental test of the equality

$$\left(\tilde{\rho} - \frac{1}{2}\right)^2 + \left(\tilde{\eta} - \frac{1}{2} \cot \alpha\right)^2 = \left(\bar{\rho} - \frac{1}{2}\right)^2 + \left(\bar{\eta} - \frac{1}{2} \cot \alpha\right)^2 \quad (16)$$

will be greatly useful at both the super- B factory and the high-luminosity LHC. It is worth mentioning that the possibility of $\alpha = \pi/2$, which is compatible with the experimental result $\alpha = (84.5^{+5.9}_{-5.2})^\circ$ extracted from $B \rightarrow \pi\pi$, $\rho\pi$ and $\rho\rho$ decay modes [15, 16], has been conjectured in exploring realistic textures of quark mass matrices or studying phenomenological implications of the CKM matrix (e.g., Refs. [17, 18, 19, 20, 21, 22, 23, 24]). In this special but suggestive case Δ'_c and Δ'_s are exactly the right triangles, from which one is left with $O = (0.5, 0)$ and $R = 0.5$ for the circular arc in Figure 1.

3 Two-loop RGE evolution of Δ'_s and Δ'_c

Note that the elements of V depend on the energy scale Λ , but they are usually treated as constants below $\Lambda = M_W$. When Λ is far above the electroweak scale $\Lambda_{\text{EW}} \sim 10^2$ GeV, the RGE running effects of V will become appreciable and should be taken into account (see Ref. [7] for a recent review). In particular, the two-loop RGEs of V have been derived for Λ evolving between Λ_{EW} and $\Lambda_{\text{GUT}} \sim 10^{16}$ GeV in the framework of the SM or its minimal supersymmetric version (MSSM) [10, 11, 12, 13]. In view of the hierarchies of quark Yukawa couplings of the same electric charge (i.e., $y_u/y_c \sim y_c/y_t \sim \lambda^4$ and $y_d/y_s \sim y_s/y_b \sim \lambda^2$ at a given energy scale [25, 26]) and the hierarchies of those off-diagonal elements of V , Barger *et al* have found [12]

$$\begin{aligned} \frac{d}{dt} \begin{pmatrix} |V_{ud}| & |V_{us}| & |V_{ub}| \\ |V_{cd}| & |V_{cs}| & |V_{cb}| \\ |V_{td}| & |V_{ts}| & |V_{tb}| \end{pmatrix} &\simeq (S_1 + S_2) \begin{pmatrix} 0 & 0 & |V_{ub}| \\ 0 & 0 & |V_{cb}| \\ |V_{td}| & |V_{ts}| & 0 \end{pmatrix}, \\ \frac{d\mathcal{J}}{dt} &\simeq 2(S_1 + S_2)\mathcal{J}, \end{aligned} \quad (17)$$

where $t \equiv \ln(\Lambda/\Lambda_{\text{EW}})$, \mathcal{J} is the well-known Jarlskog invariant of CP violation [27] and $\mathcal{J} \simeq A^2\lambda^6\eta$ holds up to the accuracy of $\mathcal{O}(\lambda^8)$, S_1 and S_2 stand respectively for the one- and two-loop contributions to the RGEs of V . To be explicit,

$$\begin{aligned} S_1 &= -\frac{1}{16\pi^2} (C_d^u y_t^2 + C_u^d y_b^2), \\ S_2 &= -\frac{1}{(16\pi^2)^2} [D_d^u y_t^2 + D_u^d y_b^2 + (D_d^{\text{ud}} + D_u^{\text{du}}) y_t^2 y_b^2 + D_d^{\text{uu}} y_t^4 + D_u^{\text{dd}} y_b^4], \end{aligned} \quad (18)$$

where y_t and y_b denote the Yukawa couplings of top and bottom quarks respectively, and the relevant coefficients on the right-hand side of Eq. (18) are

$$\begin{aligned} C_d^u = C_u^d &= -\frac{3}{2}, \quad D_d^u \simeq -\frac{79}{80}g_1^2 + \frac{9}{16}g_2^2 - 16g_3^2 + \frac{15}{4}(y_t^2 + y_b^2), \\ D_u^d &\simeq -\frac{43}{80}g_1^2 + \frac{9}{16}g_2^2 - 16g_3^2 + \frac{15}{4}(y_t^2 + y_b^2), \quad D_d^{\text{uu}} = D_u^{\text{dd}} = \frac{11}{4}, \quad D_d^{\text{ud}} = D_u^{\text{du}} = -1, \end{aligned} \quad (19)$$

in the SM ¹; or

$$\begin{aligned} C_d^u &= C_u^d = 1, & D_d^u &\simeq \frac{4}{5}g_1^2 - 3y_t^2, & D_u^d &\simeq \frac{2}{5}g_1^2 - 3y_b^2, \\ D_d^{uu} &= D_u^{dd} = -2, & D_d^{ud} &= D_u^{du} = 0, \end{aligned} \quad (20)$$

in the MSSM with g_i (for $i = 1, 2, 3$) being the respective gauge couplings of electromagnetic, weak and strong interactions. After a careful check of the approximations made in obtaining Eq. (17), we conclude that the two-loop RGEs shown in Eq. (17) are actually valid up to the accuracy of $\mathcal{O}(\lambda^4)$. To the same order, the two-loop RGEs of the Wolfenstein parameters can be figured out as follows:

$$\frac{d\lambda}{dt} \simeq \frac{d\rho}{dt} \simeq \frac{d\eta}{dt} \simeq 0, \quad \frac{dA}{dt} \simeq (S_1 + S_2)A, \quad \frac{d\bar{\rho}}{dt} \simeq \frac{d\bar{\eta}}{dt} \simeq \frac{d\tilde{\rho}}{dt} \simeq \frac{d\tilde{\eta}}{dt} \simeq 0. \quad (21)$$

Two immediate comments are in order.

- The rescaled unitarity triangles Δ'_s and Δ'_c keep unchanged when the energy scale Λ evolves from Λ_{EW} to Λ_{GUT} or vice versa, in a very good approximation up to the accuracy of $\mathcal{O}(\lambda^4)$. Accordingly, three sides of the original unitarity triangle Δ_s or Δ_c are rescaled with the same amount as Λ evolves, and thus the overall shape of either of the two triangles keeps undeformed up to the same accuracy. Although a similar observation has been made with the help of the one-loop RGEs [28], the relevant accuracy is certainly worse than the present two-loop result.
- Given $g_1 \simeq 0.46$, $g_2 \simeq 0.65$ and $g_3 \sim 1.21$ together with $y_t \simeq 1$ and $y_b \simeq y_t/60$ at $\Lambda = M_Z$ in the SM [16, 25, 26], one may make a rough but instructive estimate

$$\frac{S_2}{S_1} \sim \frac{1}{16\pi^2} \cdot \frac{D_d^u + D_d^{uu}y_t^2}{C_d^u} \sim \mathcal{O}(\lambda^2). \quad (22)$$

It is more difficult to analytically estimate the order of S_2/S_1 in the MSSM, because y_t and y_b depend on $\tan\beta$ in a different way. In Figure 2 we illustrate the magnitudes of S_1 , S_2 and S_2/S_1 changing with the energy scale Λ , where $M_H \simeq 125$ GeV in the SM and $\tan\beta \simeq 10$ or 30 in the MSSM are input. It becomes clear that the two-loop effect is suppressed by a factor of $\mathcal{O}(\lambda^3)$ to $\mathcal{O}(\lambda^2)$ in magnitude as compared with the dominant one-loop contribution, but it definitely makes sense for us to keep the former in the approximations made in Eq. (17).

Moreover, it is well known that the area of each of the six CKM unitarity triangles equals $\mathcal{J}/2$, and hence the two-loop RGE evolution of \mathcal{J} is consistent with that of A^2 in the Wolfenstein parametrization up to the accuracy of $\mathcal{O}(\lambda^4)$.

The integral form of Eq. (21) can be obtained in a straightforward way as follows:

$$\begin{aligned} \lambda(\Lambda) &\simeq \lambda(\Lambda_{\text{EW}}), & \rho(\Lambda) &\simeq \rho(\Lambda_{\text{EW}}), & \eta(\Lambda) &\simeq \eta(\Lambda_{\text{EW}}), & A(\Lambda) &\simeq I_1 I_2 A(\Lambda_{\text{EW}}); \\ \bar{\rho}(\Lambda) &\simeq \bar{\rho}(\Lambda_{\text{EW}}), & \bar{\eta}(\Lambda) &\simeq \bar{\eta}(\Lambda_{\text{EW}}), & \tilde{\rho}(\Lambda) &\simeq \tilde{\rho}(\Lambda_{\text{EW}}), & \tilde{\eta}(\Lambda) &\simeq \tilde{\eta}(\Lambda_{\text{EW}}), \end{aligned} \quad (23)$$

where Λ denotes an arbitrary energy scale between Λ_{EW} and Λ_{GUT} , and the loop functions I_i (for $i = 1, 2$) are simply defined as

$$I_i = \exp\left(\int_0^{\ln(\Lambda/\Lambda_{\text{EW}})} S_i dt\right). \quad (24)$$

¹Note that the errors associated with D_d^u and D_u^d in the SM case in Refs. [10, 12] were corrected in Ref. [13].

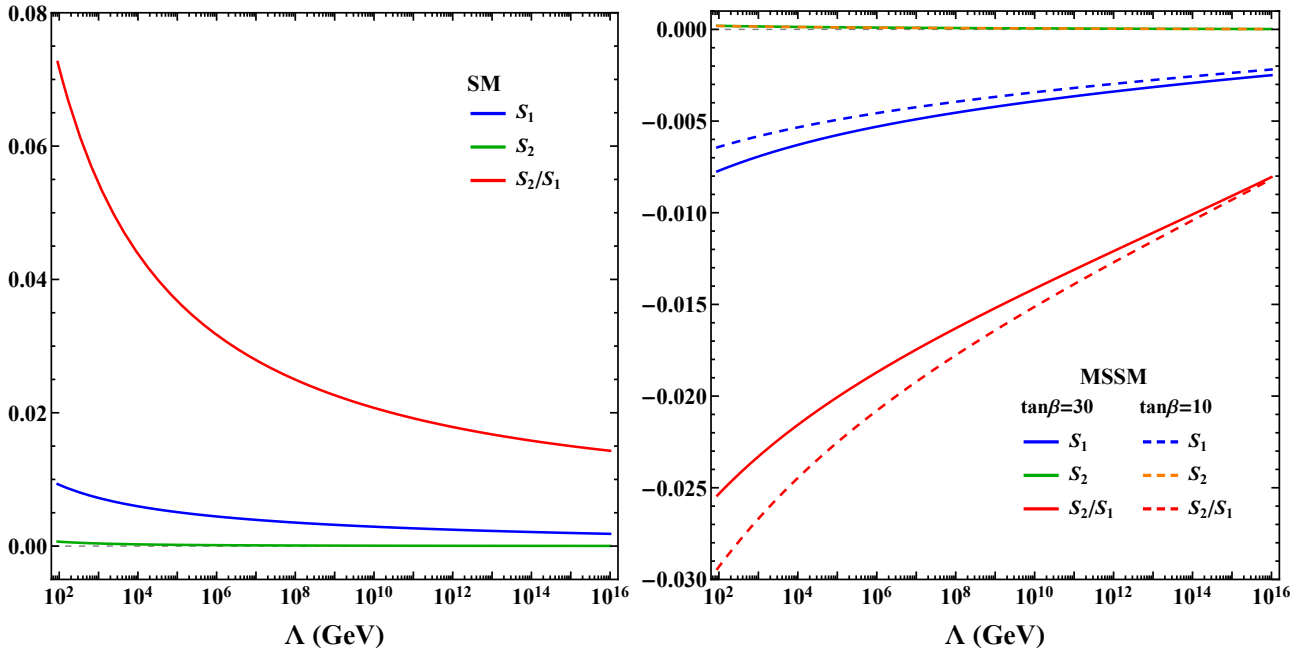


Figure 2: A comparison between one- and two-loop contributions to the RGEs in Eq. (17) in the SM with $M_H \simeq 125$ GeV (left panel) and the MSSM with $\tan \beta = 10$ or 30 (right panel).

Of course, $|V_{ub}|$, $|V_{cb}|$, $|V_{td}|$ and $|V_{ts}|$ evolve in the same way as A , while $\mathcal{J}(\Lambda) \simeq I_1^2 I_2^2 \mathcal{J}(\Lambda_{EW})$ holds for the Jarlskog invariant. In comparison, $|V_{ud}|$, $|V_{us}|$, $|V_{cd}|$, $|V_{cs}|$ and $|V_{tb}|$ are essentially stable against changes of the energy scale Λ .

For the sake of illustration, we show the running behaviors of I_1 , I_2 and $I_1 I_2$ in Figure 2, where $M_H \simeq 125$ GeV has been input for the SM and $\tan \beta = 10$ or 30 has been taken for the MSSM. One can see that the overall RGE-induced scaling effect on A from Λ_{EW} and Λ_{GUT} or vice versa is about 10% for the inputs under consideration.

4 Comments on leptonic unitarity triangles

In the lepton sector, the 3×3 Pontecorvo-Maki-Nakagawa-Sakata (PMNS) flavor mixing matrix U [29, 30] can geometrically be described by three pairs of unitarity triangles in the complex plane [6]². Here we focus on the rescaled versions of these triangles, defined as

$$\begin{aligned} \Delta'_e : 1 + \frac{U_{\mu 2} U_{\tau 2}^*}{U_{\mu 1} U_{\tau 1}^*} + \frac{U_{\mu 3} U_{\tau 3}^*}{U_{\mu 1} U_{\tau 1}^*} &= 0, \\ \Delta'_1 : 1 + \frac{U_{\mu 3} U_{\mu 2}^*}{U_{e 3} U_{e 2}^*} + \frac{U_{\tau 3} U_{\tau 2}^*}{U_{e 3} U_{e 2}^*} &= 0, \end{aligned} \quad (25)$$

$$\begin{aligned} \Delta'_\mu : 1 + \frac{U_{\tau 1} U_{e 1}^*}{U_{\tau 2} U_{e 2}^*} + \frac{U_{\tau 3} U_{e 3}^*}{U_{\tau 2} U_{e 2}^*} &= 0, \\ \Delta'_2 : 1 + \frac{U_{e 1} U_{e 3}^*}{U_{\mu 1} U_{\mu 3}^*} + \frac{U_{\tau 1} U_{\tau 3}^*}{U_{\mu 1} U_{\mu 3}^*} &= 0, \end{aligned} \quad (26)$$

²Note that whether the PMNS matrix U is exactly unitary or not depends the mechanism of neutrino mass generation, but its possible unitarity-violating effects must be less than one percent as constrained by current precision electroweak data and neutrino oscillation data [7].

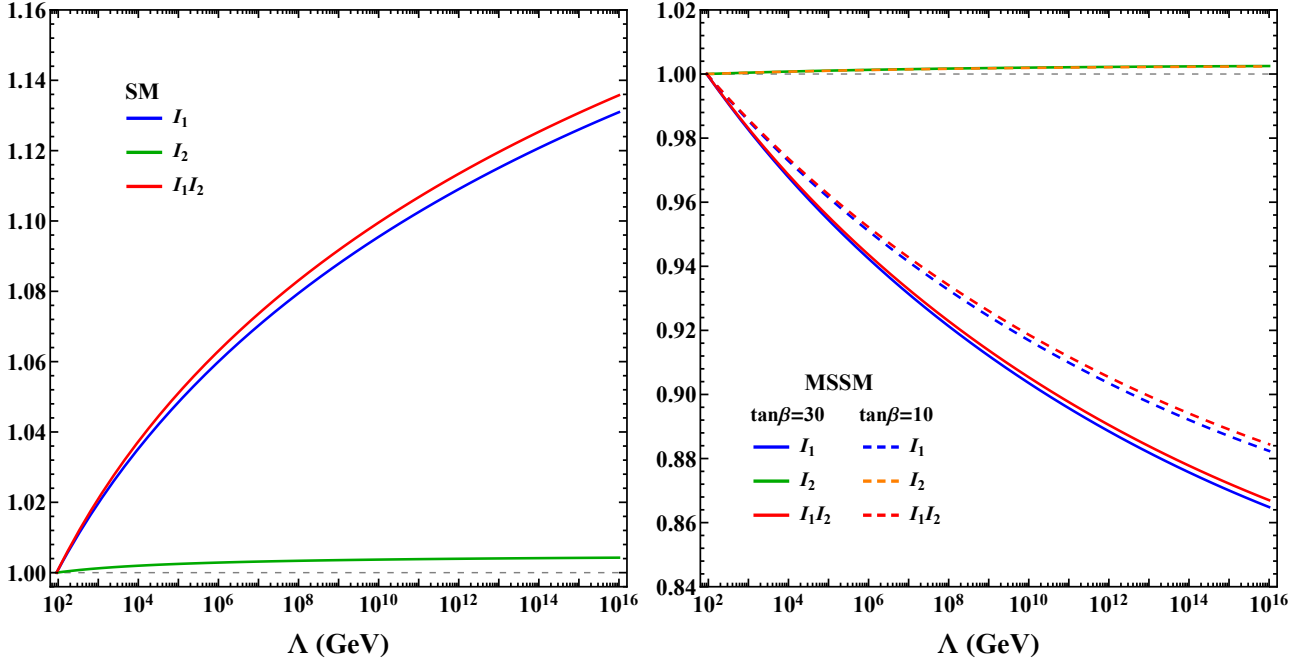


Figure 3: The two-loop RGE evolution functions I_1 , I_2 and $I_1 I_2$ in the SM with $M_H \simeq 125$ GeV (left panel) and the MSSM with $\tan \beta = 10$ or 30 (right panel).

and

$$\begin{aligned} \Delta'_\tau : 1 + \frac{U_{e1} U_{\mu 1}^*}{U_{e3} U_{\mu 3}^*} + \frac{U_{e2} U_{\mu 2}^*}{U_{e3} U_{\mu 3}^*} &= 0, \\ \Delta'_3 : 1 + \frac{U_{e2} U_{e1}^*}{U_{\tau 2} U_{\tau 1}^*} + \frac{U_{\mu 2} U_{\mu 1}^*}{U_{\tau 2} U_{\tau 1}^*} &= 0, \end{aligned} \quad (27)$$

where $U_{\alpha i}$ ($\alpha = e, \mu, \tau$ and $i = 1, 2, 3$) are the elements of the PMNS matrix. Note that these six rescaled triangles are completely insensitive to the Majorana phases of U . Note also that each pair of the PMNS unitarity triangles share a common inner angle, which can be defined as follows:

$$\begin{aligned} \alpha_e &\equiv \arg \left(-\frac{U_{\mu 2} U_{\tau 2}^*}{U_{\mu 3} U_{\tau 3}^*} \right) = \arg \left(-\frac{U_{\tau 3} U_{\tau 2}^*}{U_{\mu 3} U_{\mu 2}^*} \right) \equiv \alpha_1, \\ \alpha_\mu &\equiv \arg \left(-\frac{U_{\tau 3} U_{e3}^*}{U_{\tau 1} U_{e1}^*} \right) = \arg \left(-\frac{U_{e1} U_{e3}^*}{U_{\tau 1} U_{\tau 3}^*} \right) \equiv \alpha_2, \\ \alpha_\tau &\equiv \arg \left(-\frac{U_{e1} U_{\mu 1}^*}{U_{e2} U_{\mu 2}^*} \right) = \arg \left(-\frac{U_{\mu 2} U_{\mu 1}^*}{U_{e2} U_{e1}^*} \right) \equiv \alpha_3, \end{aligned} \quad (28)$$

In a way similar to Eqs. (3) and (4) for the two b -flavored unitarity triangles, one may define vertices of the above six PMNS unitarity triangles in the complex plane:

$$\begin{aligned} \rho_e + i\eta_e &= -\frac{U_{\mu 3} U_{\tau 3}^*}{U_{\mu 1} U_{\tau 1}^*}, & \rho_1 + i\eta_1 &= -\frac{U_{\mu 3} U_{\mu 2}^*}{U_{e3} U_{e2}^*}, \\ \rho_\mu + i\eta_\mu &= -\frac{U_{\tau 1} U_{e1}^*}{U_{\tau 2} U_{e2}^*}, & \rho_2 + i\eta_2 &= -\frac{U_{\tau 1} U_{\tau 3}^*}{U_{\mu 1} U_{\mu 3}^*}, \\ \rho_\tau + i\eta_\tau &= -\frac{U_{e2} U_{\mu 2}^*}{U_{e3} U_{\mu 3}^*}, & \rho_3 + i\eta_3 &= -\frac{U_{e2} U_{e1}^*}{U_{\tau 2} U_{\tau 1}^*}. \end{aligned} \quad (29)$$

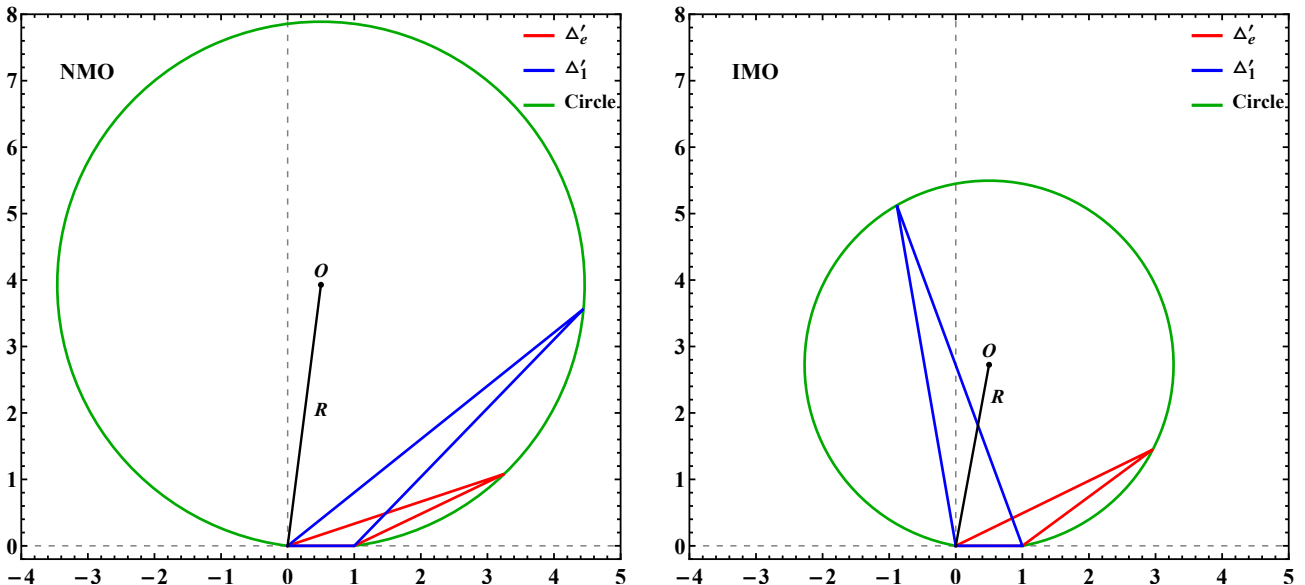


Figure 4: The rescaled PMNS unitarity triangles Δ'_e and Δ'_1 in the complex plane for either the normal neutrino mass ordering (left panel) or the inverted mass ordering (right panel).

Then Eq. (28) allows us to show that vertices (ρ_e, η_e) and (ρ_1, η_1) must be located on a circular arc, whose center and radius are given by $O = (0.5, 0.5 \cot \alpha_e)$ and $R = 0.5 \csc \alpha_e$ respectively:

$$\left(\rho_e - \frac{1}{2}\right)^2 + \left(\eta_e - \frac{1}{2} \cot \alpha_e\right)^2 = \left(\rho_1 - \frac{1}{2}\right)^2 + \left(\eta_1 - \frac{1}{2} \cot \alpha_e\right)^2 = \left(\frac{1}{2} \csc \alpha_e\right)^2. \quad (30)$$

Of course, vertices (ρ_μ, η_μ) and (ρ_2, η_2) are also on a circular arc defined by $O = (0.5, 0.5 \cot \alpha_\mu)$ and $R = 0.5 \csc \alpha_\mu$, and vertices (ρ_τ, η_τ) and (ρ_3, η_3) are located on another circular arc with $O = (0.5, 0.5 \cot \alpha_\tau)$ and $R = 0.5 \csc \alpha_\tau$. Unlike the CKM matrix V discussed above, the PMNS matrix U does not have a strong hierarchy in its structure, and hence it is difficult to make an expansion of U in powers of a small parameter [31].

To illustrate, we plot each pair of the rescaled PMNS unitarity triangles in the complex plane in Figures 4–6 and calculate not only the center and radius of the circular arc on which they are located but also their common inner angle in Table 1 by using the best-fit values of three neutrino mixing angles (θ_{12} , θ_{13} and θ_{23}) and the Dirac CP-violating phase (δ) [32, 33], where both the normal neutrino mass ordering (NMO) and the inverted mass ordering (IMO) are taken into account. We admit that for the time being the large uncertainty associated with δ prevents us from establishing the leptonic unitarity triangles in a reliable way [34, 35], but Figures 4–6 and Table 1 do give one a ball-park feeling of some salient features of unitarity triangles in the lepton sector. In particular, it seems much easier for us to distinguish between each pair of the rescaled PMNS unitarity triangles on a circular arc, simply because their shapes and vertices are quite different. But this observation might change once more precise data are available.

5 Summary

Motivated by the prospects that the *twin* CKM unitarity triangles Δ_s and Δ_c will be precisely measured at the super- B factory and the high-luminosity LHC in the coming years, we address the question of whether they can be experimentally distinguished from each other. With the help of the Wolfenstein parameters, we have calculated the vertex $(\bar{\rho}, \bar{\eta})$ of Δ'_s and the vertex

Table 1: Numerical results for the center O and radius R of a circular arc on which each pair of the PMNS unitarity triangles are located, and those for their common inner angle α_i (for $i = 1, 2, 3$) defined in Eq. (28) in the NMO or IMO case, where the best-fit values of three neutrino mixing angles and the Dirac CP-violating phase [32, 33] have been input.

| Triangles | Normal mass ordering (NMO) | | | Inverted mass ordering (IMO) | | |
|--------------------|----------------------------|------------|------------------------|------------------------------|------------|------------------------|
| | Center O | Radius R | Inner angle α_i | Center O | Radius R | Inner angle α_i |
| $\Delta'_{e,1}$ | (0.5, 3.93) | 3.96 | 7.25° | (0.5, 2.72) | 2.77 | 10.40° |
| $\Delta'_{\mu,2}$ | (0.5, 0.74) | 0.89 | 34.11° | (0.5, -0.01) | 0.50 | 90.88° |
| $\Delta'_{\tau,3}$ | (0.5, 2.04) | 2.10 | 13.76° | (0.5, 1.62) | 1.70 | 17.16° |

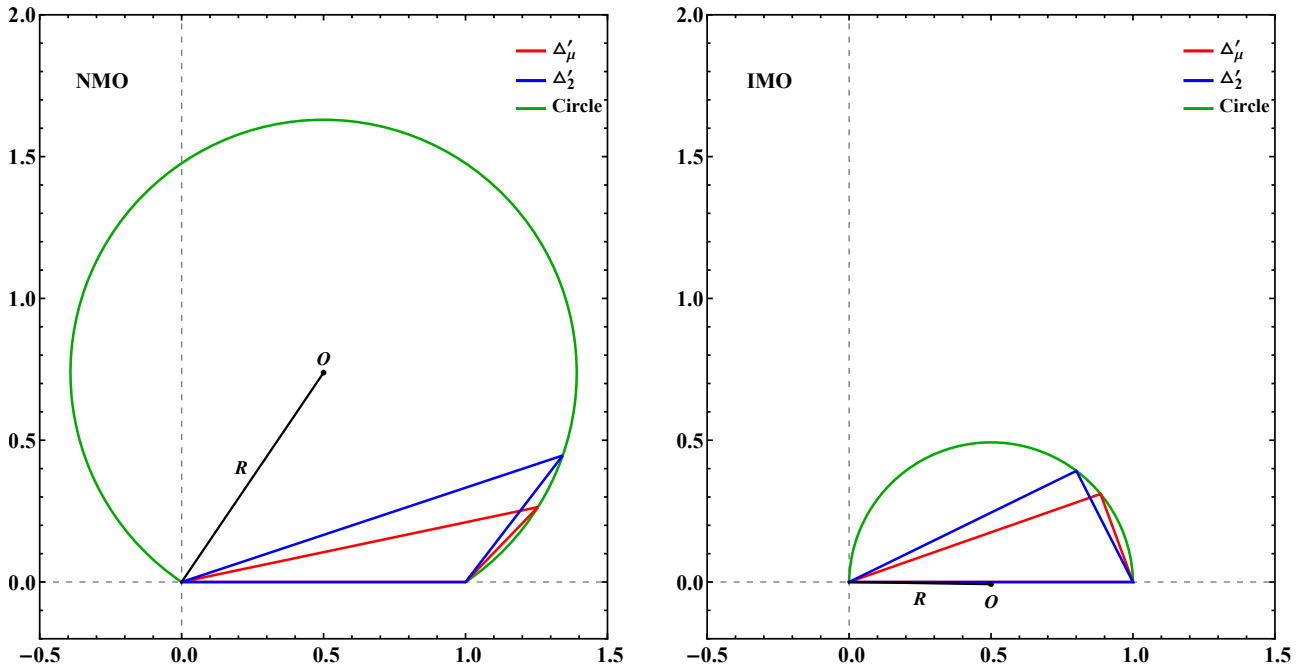


Figure 5: The rescaled PMNS unitarity triangles Δ'_μ and Δ'_2 in the complex plane for either the normal neutrino mass ordering (left panel) or the inverted mass ordering (right panel).

$(\tilde{\rho}, \tilde{\eta})$ of Δ'_c — the rescaled versions of Δ_s and Δ_c in the complex plane — and their inner angles up to the accuracy of $\mathcal{O}(\lambda^6)$. In particular, we find that the two vertices are actually located on a circular arc, whose center and radius are given by $O = (0.5, 0.5 \cot \alpha)$ and $R = 0.5 \csc \alpha$ respectively. Both $\tilde{\rho} - \bar{\rho}$ and $\tilde{\eta} - \bar{\eta}$ are found to be of $\mathcal{O}(\lambda^2)$, so Δ'_c and Δ'_s are expected to be experimentally distinguishable if their vertices can be measured at the 1% precision level. We have pointed out that a similar experimental sensitivity will allow us to probe small differences between the inner angles of Δ'_c and Δ'_s . We have also shown that $(\bar{\rho}, \bar{\eta})$ and $(\tilde{\rho}, \tilde{\eta})$ are insensitive to the two-loop RGE running effects up to the accuracy of $\mathcal{O}(\lambda^4)$, and this observation implies that the shapes of Δ_c and Δ_s keep invariant up to the same accuracy when the energy scale Λ changes between $\Lambda_{\text{EW}} \sim 10^2$ GeV and $\Lambda_{\text{GUT}} \sim 10^{16}$ GeV. As a consequence, the experimental results of all the inner angles of Δ_c and Δ_s obtained at low energies can directly be confronted with some theoretical predictions at a superhigh energy scale.

As a by-product, three pairs of the rescaled PMNS unitarity triangles in the lepton sector have been discussed in a similar but brief way. The vertices of each pair of the triangles are also located on a circular arc, but we find that their shapes look quite different if only the best-fit values of lepton flavor mixing parameters are taken into account. Once the Dirac CP-violating

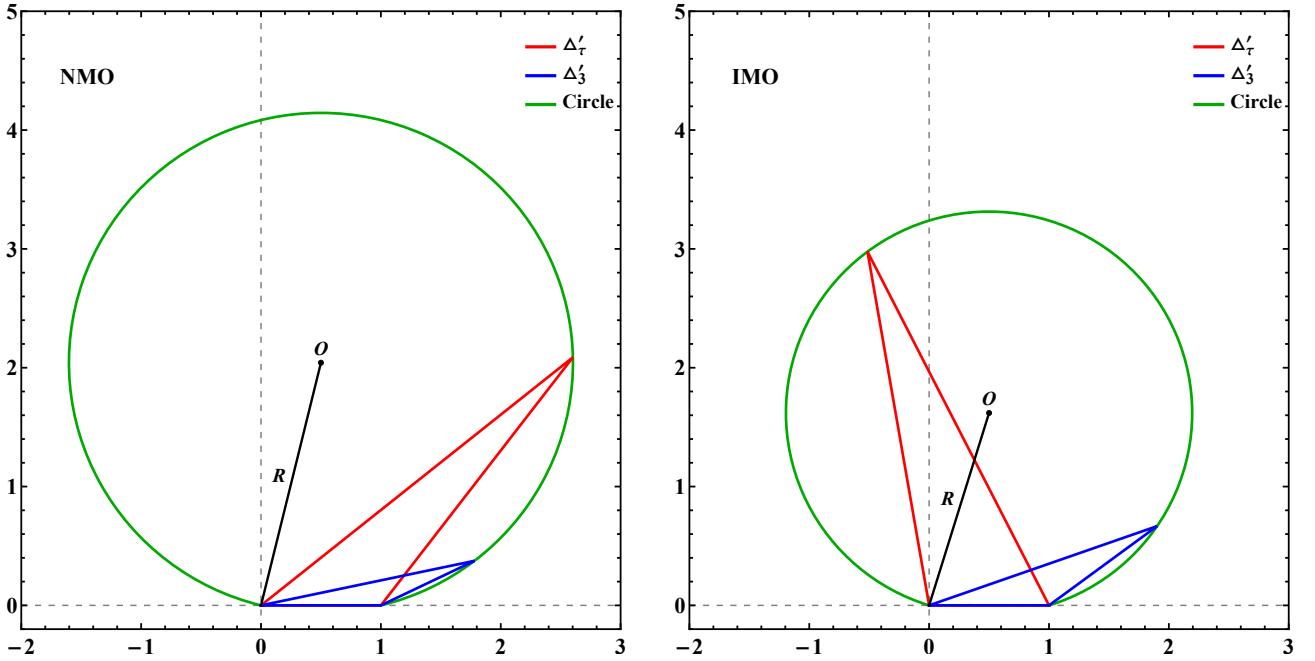


Figure 6: The rescaled PMNS unitarity triangles Δ'_τ and Δ'_3 in the complex plane for either the normal neutrino mass ordering (left panel) or the inverted mass ordering (right panel).

phase δ is reliably determined in the upcoming long-baseline neutrino oscillation experiments, it will be possible to systematically study the PMNS unitarity triangles³. In this respect we expect that the geometrical language under discussion may be very helpful to test consistency of the PMNS picture for lepton flavor mixing and CP violation and look for possible deviations caused by new physics associated with the origin of tiny neutrino masses.

Acknowledgements

One of us (Z.Z.X.) is deeply indebted to his schoolmate (A.J.) at Peking University for motivating him to pay particular attention to all the twin phenomena in physics and beyond since 1984. This work was supported in part by the National Natural Science Foundation of China under grant No. 11775231 and grant No. 11835013.

³Private communications with Shun Zhou.

References

- [1] E. Kou *et al.* [Belle-II Collaboration], The Belle II Physics Book, arXiv:1808.10567 [hep-ex].
- [2] M. Bona *et al.* [SuperB Collaboration], SuperB: A High-Luminosity Asymmetric $e^+ e^-$ Super Flavor Factory. Conceptual Design Report, arXiv:0709.0451 [hep-ex].
- [3] R. Aaij *et al.* [LHCb Collaboration], Physics case for an LHCb Upgrade II - Opportunities in flavour physics, and beyond, in the HL-LHC era, arXiv:1808.08865.
- [4] N. Cabibbo, Unitary Symmetry and Leptonic Decays, Phys. Rev. Lett. **10** (1963) 531.
- [5] M. Kobayashi and T. Maskawa, CP Violation in the Renormalizable Theory of Weak Interaction, Prog. Theor. Phys. **49** (1973) 652.
- [6] H. Fritzsch and Z. z. Xing, Mass and flavor mixing schemes of quarks and leptons, Prog. Part. Nucl. Phys. **45** (2000) 1 [hep-ph/9912358].
- [7] Z. z. Xing, Flavor structures of charged fermions and massive neutrinos, arXiv:1909.09610 [hep-ph].
- [8] I. I. Y. Bigi and A. I. Sanda, On the other five KM triangles, hep-ph/9909479.
- [9] L. Wolfenstein, Parametrization of the Kobayashi-Maskawa Matrix, Phys. Rev. Lett. **51** (1983) 1945.
- [10] M. E. Machacek and M. T. Vaughn, Two Loop Renormalization Group Equations in a General Quantum Field Theory. 2. Yukawa Couplings, Nucl. Phys. B **236** (1984) 221.
- [11] V. D. Barger, M. S. Berger and P. Ohmann, Supersymmetric grand unified theories: Two loop evolution of gauge and Yukawa couplings, Phys. Rev. D **47** (1993) 1093 [hep-ph/9209232].
- [12] V. D. Barger, M. S. Berger and P. Ohmann, Universal evolution of CKM matrix elements, Phys. Rev. D **47** (1993) 2038 [hep-ph/9210260].
- [13] M. x. Luo and Y. Xiao, Two loop renormalization group equations in the standard model, Phys. Rev. Lett. **90** (2003) 011601 [hep-ph/0207271].
- [14] A. J. Buras, M. E. Lautenbacher and G. Ostermaier, Waiting for the top quark mass, $K^+ \rightarrow \pi^+ \nu \bar{\nu}$, $B_s^0 - \bar{B}_s^0$ mixing and CP asymmetries in B decays, Phys. Rev. D **50** (1994) 3433 [hep-ph/9403384].
- [15] J. Charles *et al.* [CKMfitter Group], CP violation and the CKM matrix: Assessing the impact of the asymmetric B factories, Eur. Phys. J. C **41** (2005) 1 [hep-ph/0406184].
- [16] M. Tanabashi *et al.* [Particle Data Group], Review of Particle Physics, Phys. Rev. D **98**, no. 3, 030001 (2018).
- [17] H. Fritzsch and Z. z. Xing, A Symmetry pattern of maximal CP violation and a determination of the unitarity triangle, Phys. Lett. B **353** (1995) 114 [hep-ph/9502297].
- [18] H. Fritzsch and Z. z. Xing, The Light quark sector, CP violation, and the unitarity triangle, Nucl. Phys. B **556** (1999) 49 [hep-ph/9904286].
- [19] H. Fritzsch and Z. z. Xing, Four zero texture of Hermitian quark mass matrices and current experimental tests, Phys. Lett. B **555** (2003) 63 [hep-ph/0212195].
- [20] Y. Koide, Maximal CP violation hypothesis and phase convention of the CKM matrix, Phys. Lett. B **607** (2005) 123 [hep-ph/0411280].
- [21] I. Masina and C. A. Savoy, Real and imaginary elements of fermion mass matrices, Nucl. Phys. B **755** (2006) 1 [hep-ph/0603101].
- [22] P. F. Harrison, D. R. J. Roythorne and W. G. Scott, Plaquette invariants and the flavour symmetric description of quark and neutrino mixings, Phys. Lett. B **657** (2007) 210 [arXiv:0709.1439 [hep-ph]].

- [23] Z. z. Xing, Right Unitarity Triangles, Stable CP-violating Phases and Approximate Quark-Lepton Complementarity, *Phys. Lett. B* **679** (2009) 111 [arXiv:0904.3172 [hep-ph]].
- [24] S. Antusch, S. F. King, M. Malinsky and M. Spinrath, Quark mixing sum rules and the right unitarity triangle, *Phys. Rev. D* **81** (2010) 033008 [arXiv:0910.5127 [hep-ph]].
- [25] Z. z. Xing, H. Zhang and S. Zhou, Updated Values of Running Quark and Lepton Masses, *Phys. Rev. D* **77** (2008) 113016 [arXiv:0712.1419 [hep-ph]].
- [26] Z. z. Xing, H. Zhang and S. Zhou, Impacts of the Higgs mass on vacuum stability, running fermion masses and two-body Higgs decays, *Phys. Rev. D* **86** (2012) 013013 [arXiv:1112.3112 [hep-ph]].
- [27] C. Jarlskog, Commutator of the Quark Mass Matrices in the Standard Electroweak Model and a Measure of Maximal CP Violation, *Phys. Rev. Lett.* **55** (1985) 1039.
- [28] S. Luo and Z. z. Xing, Radiative Corrections to the CKM Unitarity Triangles, *J. Phys. G* **37** (2010) 075018 [arXiv:0912.4593 [hep-ph]].
- [29] Z. Maki, M. Nakagawa and S. Sakata, Remarks on the unified model of elementary particles, *Prog. Theor. Phys.* **28** (1962) 870.
- [30] B. Pontecorvo, Neutrino Experiments and the Problem of Conservation of Leptonic Charge, *Sov. Phys. JETP* **26** (1968) 984 [*Zh. Eksp. Teor. Fiz.* **53** (1967) 1717].
- [31] Z. z. Xing, Wolfenstein - like parametrization of the neutrino mixing matrix, *J. Phys. G* **29** (2003) 2227 [hep-ph/0211465].
- [32] F. Capozzi, E. Lisi, A. Marrone and A. Palazzo, Current unknowns in the three neutrino framework, *Prog. Part. Nucl. Phys.* **102** (2018) 48 [arXiv:1804.09678 [hep-ph]].
- [33] I. Esteban, M. C. Gonzalez-Garcia, A. Hernandez-Cabezudo, M. Maltoni and T. Schwetz, Global analysis of three-flavour neutrino oscillations: synergies and tensions in the determination of θ_{23} , δ_{CP} , and the mass ordering, *JHEP* **1901**, 106 (2019) [arXiv:1811.05487 [hep-ph]].
- [34] M. C. Gonzalez-Garcia, M. Maltoni and T. Schwetz, Updated fit to three neutrino mixing: status of leptonic CP violation, *JHEP* **1411** (2014) 052 [arXiv:1409.5439 [hep-ph]].
- [35] Z. z. Xing and J. y. Zhu, Leptonic Unitarity Triangles and Effective Mass Triangles of the Majorana Neutrinos, *Nucl. Phys. B* **908** (2016) 302 [arXiv:1511.00450 [hep-ph]].